Hydrophilic and Double Hydrophilic/Hydrophobic Microcapsules using a Single, Thermally Responsive, Self-Sorting Dispersant

Lérys Granado [1,2,3,4], Céline Burel [1], Rémi Giordanengo [1], Ahmed Alsayed [1], Denis Bendejacq[1] and François Ganachaud [1,2,3,4]*

[1] Complex Assemblies of Soft Matter, UMI 3254, Solvay/CNRS/Upenn, 350 George Patterson Boulevard, Bristol, Pennsylvania, 19007, United States

[2] Laboratory for Research on the Structure of Matter, University of Pennsylvania, Philadelphia, Pennsylvania, 19104, United States

[3] CNRS, UMR 5223, Ingénierie des Matériaux Polymères, Villeurbanne, 69621, France

[4] INSA-Lyon, Ingénierie des Matériaux Polymères, Villeurbanne, 69621, France

* Correspondence: francois.ganachaud@insa-lyon.fr.

Supporting Information Available

ABSTRACT: Encapsulating and storing hydrophilic payloads are still challenging nowadays Here, a simple pathway is described to generate different water-filled microcapsule dispersions. We carefully chose a unique polyvinyl alcohol (PVA) dispersant that is able to stabilize and cover both direct and inverse interfaces. Single hollow capsules consisting of precipitated PVA shells were first prepared in one pot. Cargo release was shown to vary from fast kinetics (pristine microcapsules) to a diffusion-controlled one (cross-linked microcapsules) after an initial burst. We then describe an extremely easy process to generate double microcapsules, which complexity was visualized by different fluorescent markers under a microscope.

The microencapsulation of hydrophilic molecules is an active soft matter research topic that finds applications in pharmaceutical,[1] cosmetic and food industries, nanomedicine,[2] surface disinfection, water treatment and so on. Yet, water-soluble molecules are generally more difficult to encapsulate than lipophilic actives.[3,4] For instance, polymersomes (made of block-copolymers) lead to diluted dispersions of nanocapsules showing low encapsulation yields and poor colloidal stability in complex formulations.[5,6] Other capsules' preparation by a three-step technique (phase inversion, polymerization and redispersion in water) engages numerous chemicals and requires high skills in soft matter chemistry.[7] There is thus clearly a need for a simple and straightforward technique for generating water-filled capsules.

Polyvinyl alcohol is a largely available, cost-effective and biocompatible water-soluble dispersant.[8] It has been widely used, albeit almost exclusively for oil-in-water (o/w) encapsulation, thanks to its unique properties. First, partially hydrolyzed PVAs, copolymers of vinyl alcohol and vinyl acetate units, exhibit a LCST in salted water, that depends mainly on the degree of hydrolysis[9] and blockiness.[10] PVA precipitates to form coacervated[11] shells at interfaces with water, and in specific conditions, even partially crystallized shells[12]. PVA also bears numerous hydroxyl groups that can react with a large variety of chemicals so as to functionalize and/or crosslink chains.[13] Last but not least, a recent study has shown that commercial PVAs of increasing molar masses present decreased HLBs[14] values as low as 6 for which inverse emulsions are stabilized.

To our knowledge, only two teams have reported the synthesis of water-filled PVA-decorated capsules made from complex formulations and by multistep inverse[15] or double emulsion[14] processes. In contrast, the present investigation reports on a simple one-pot preparation of surfactant-free hydrophilic molecule-loaded microcapsules. The principle of this approach (Fig 1) lies in the use of a single, thermo-responsive PVA that can thermally switch the curvature between water and a hydrophobic organic solvent phases (referred to hereafter as 'oil'). When an oil and an aqueous PVA solution are emulsified above the dispersant LCST, water-in-oil (w/o) dispersions are formed. Yet, coming back to room temperature, the same polymer stabilizes the capsules redispersed in the water continuous phase. Starting from w/o dispersions, two pathways are then conceivable. (1) Microcapsules readily formed by coacervation of PVA at high temperature are transferred to water (with or without an intermediate covalent crosslinking step). (2) The coacervate is involved in a second emulsification step performed below PVA's LCST, by adding the same aqueous polymer solution. This yields the creation of multiple dispersions, in a remarkably simple manner (see experimental details in Table S1 of the supplementary information).

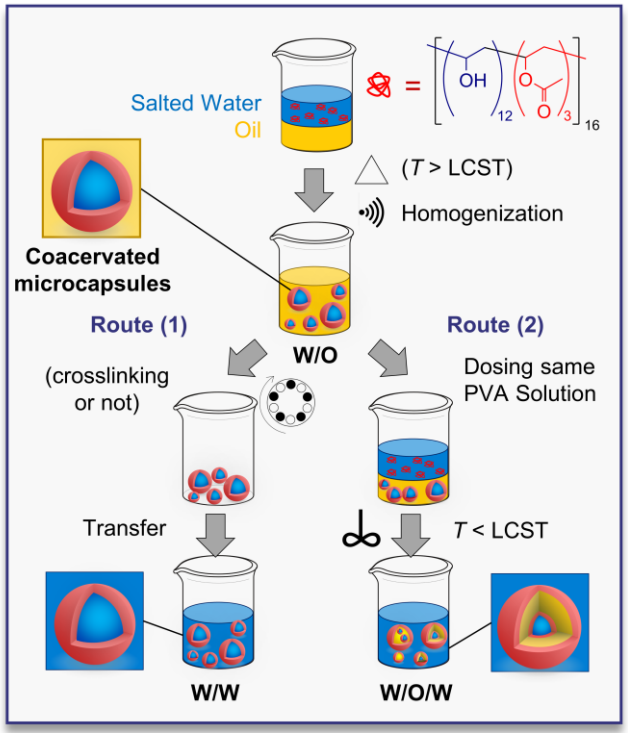

Figure 1. Conceptual scheme recapitalizing the approach of this study.

A preliminary screening of different hydrolyzed PVAs, in the range of 55-98% hydrolyzed units, showed that only one candidate, a copolymer of 80% hydrolyzed units and M_w of 9.8 kg mol^{-1}, was able to stabilize both o/w and w/o dispersions at low and high temperatures, respectively (see Table S2). This particular polyvinyl alcohol, referred to as PVA\80-10 in the following, was selected to carry on this study (Fig 1). Owing to the fact that the polymer microstructure greatly impacts its behavior in solution, we carried out microstructural and physicochemical analyses of PVA\80-10 (Fig S1-S4). The main characteristics are reported in Table 1. PVA\80-10's LCST in salted water (0.1 M sodium sulfate) ranges between 38 °C and 52 °C depending on its concentration (Fig 2a and Fig S5). Below LCST, this PVA is totally soluble in salted water yielding transparent solution. On the other hand, it generates pseudo-micelles above the LCST, thanks to its blockiness. Previous authors proposed that these pseudo-micelles are constituted of an acetate-rich core surrounded by loops of alcohol-rich polymer segments[16]. At the LCST, the interfacial tension between oil and PVA\80-10 aqueous solution shows an abrupt drop, as the result of polymer precipitation (Fig S6).

When PVA aqueous solution and chloroform – chosen as a conveniently volatile oil – are emulsified below and above the LCST, this yields o/w and w/o dispersions, respectively. Both dispersions are stabilized by the same PVA\80-10, in all proportions (Fig 2b). The process is remarkably easy (refer to the experimental details and movies in SI). The natures of the continuous and discrete phases are confirmed by fluorescence confocal microscopy images, showing hydrophilic domains in Fig 2c-d. These dispersions are stable for more than six months.

Table 1. Properties of PVA\80-10 used in this study.

Properties	Values
M_w[1]	9.8 kg mol^{-1}
$Đ$[1]	1.09
Hydrolysis Degree[2]	80%
Av. alcohol sequence[2]	12.3 monomers
Av. acetate sequence[2]	3.0 monomers
Blockiness index, η[2]	0.41 (= mostly blocky)
Tacticity, P_m[2]	0.51 (= mostly atactic)
T_g[3]	65 °C
T_m[3]	150 °C
Crystallinity[3,4]	34-40%
Residual water content[3]	4-5 wt%

[1] Determined using gel permeation chromatography. [2] Determined using quantitative ^{13}C nuclear magnetic resonance (NMR) in D_2O (Fig S1-S2). [3] Determined using differential scanning calorimetry (Fig S3).[4] Determined using X-ray diffraction (XRD) on as-received powder (Fig S4).

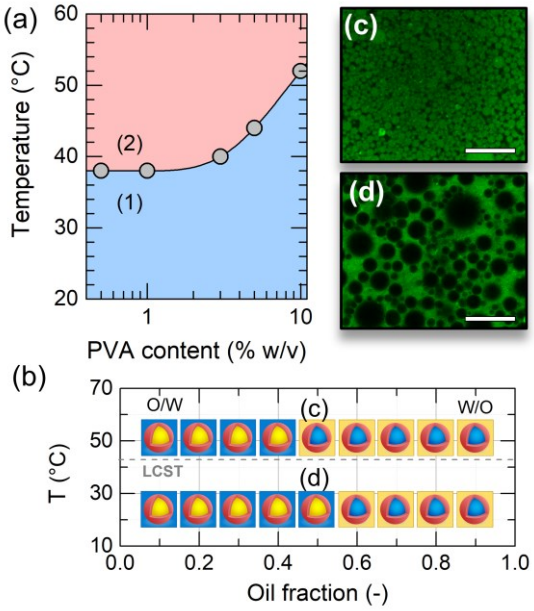

Figure 2. (a) Phase diagram of PVA\80-10 in 0.1 M sodium sulfate aqueous solution, as a function of PVA concentration as measured by dynamic light scattering (Fig S5), zones (1) and (2) indicate the domains where PVA\80-10 is totally solvated and where PVA\80-10 forms pseudo-micelles, respectively. (b) Phase diagram showing the type of emulsions generated as a function of temperature (25 °C and 50 °C) and chloroform fraction (respectively to PVA 5% w/v in 0.1 M sodium sulfate aqueous solution). According fluorescence microscopy images using hydrophilic fluorophore showing (c) water-in-oil and (d) oil-in-water dispersions (oil:water, 50:50, v:v). Scale-bars represent 50 μm.

Following the route (1) of Fig 1, w/o dispersions were first prepared by high shear homogenization at 50 °C. The coacervated capsules were separated from the organic continuous phase by centrifugation (eased by the large density difference between water and chloroform). The pristine water-filled capsules were readily dispersed in salted water, to yield a colloidally stable water-in-water (w/w) dispersion (Fig 3a-b). The typical size of w/w microcapsules was determined using image analysis (Fig 3c). The number-average microcapsule diameter was estimated at 1.5 μm, with a polydispersity index of 0.56. Different sizes of capsules are achievable according to the homogenization technique: (i) 1.5 μm-wide capsules using either sonication or high shear homogenizer (25,000 rpm, Fig 3a-b) and (ii) 6.7 μm-wide capsules by low shear homogenizer (5000 rpm, Fig 3c).

The hollow character of the microcapsules was confirmed by fluorescence microscopy analysis of dye-tagged PVA\80-10 constituting the shell of microcapsules (Fig 3d). From image analysis, e.g. in Fig 3e and Table S3, the typical shell thickness in water was estimated at around 0.8 μm. Remarkably, most of the uncrosslinked pristine capsules sustain the transfer in aqueous solution, salted or not, and remain structured over several months, in absence of shear (see Fig 3b). This counter-intuitive finding can be explained by the probable numerous intermolecular hydrogen bonds between PVA chains giving a resilient capsule shell. XRD of w/o dispersions did not show any crystallization of the polymer shell (Fig S4).

The pristine capsules were dried from the w/o state and analyzed under scanning electron microscopy (SEM). Fig 3e shows typical SEM micrographs. Remarkably, most capsules sustain low vacuum conditions, again despite the absence of crosslinking. Some microcapsules present uneven surfaces, as shown in the inset of Fig 3e.

To strengthen the microcapsule shell, PVA\80-10 chains were crosslinked using glutaraldehyde. The reaction is specific to 1,3 diol motif of PVA and catalyzed by Brønsted acids, yielding bis-acetals (Fig 3f). The reaction was performed in the w/o state, adding the crosslinker in the continuous phase. The crosslinking kinetics was followed by ^{1}H NMR (Fig S8). From the kinetic profile in Fig 3h, one observes that the reaction performed at 50 °C reaches completion after nearly two hours. The optimum stoichiometric amount of crosslinker was found

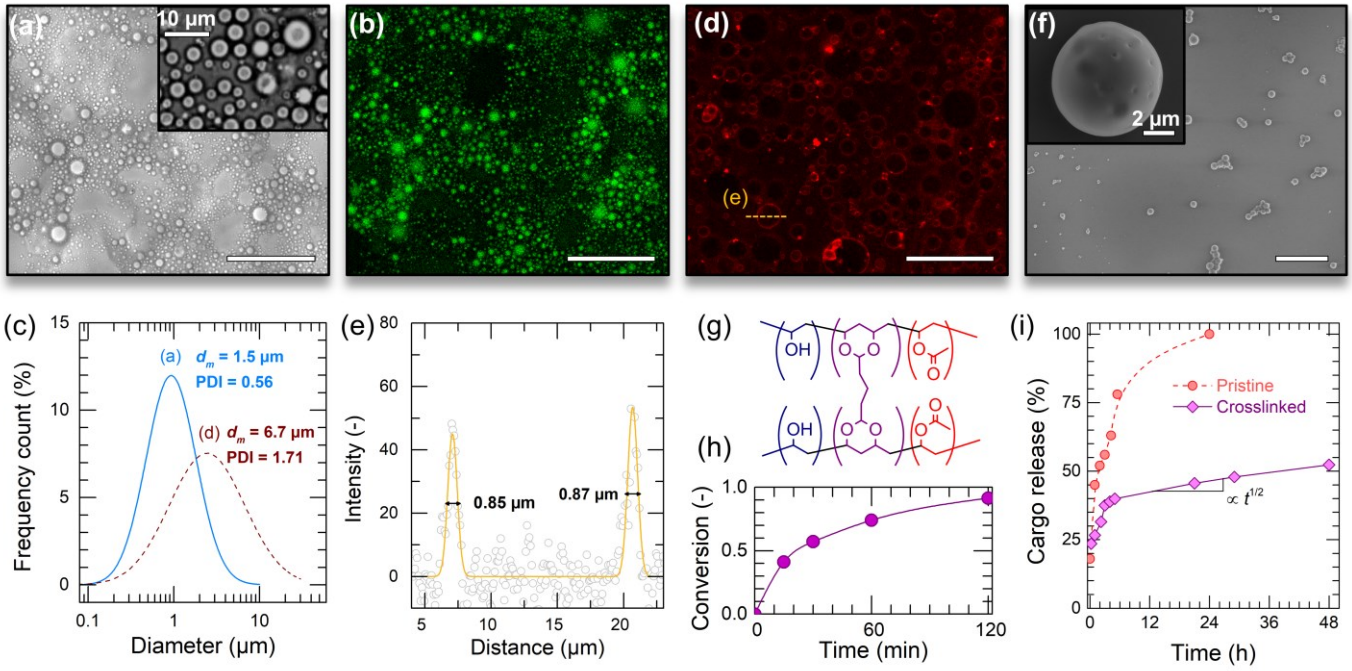

Figure 3. (a) Transmission confocal microscopy image showing hydrophilic dye-loaded microcapsules in water (inset: zoom acquired on a conventional microscope) and (b) corresponding confocal fluorescence image (capsules obtained with a homogenization at 25 000 rpm for 30 min). (c) Typical log normal diameter distribution of microcapsules in water, according to images (a) and (d), cf. experimental data in Fig S7. (d) Fluorescence confocal microscopy image of microcapsules in water from tagged-PVA to show the inner-water morphology of the spheres and assess shell thickness measurements (homogenization at 5 000 rpm for 5 min). (e) A typical profile of light intensity of a PVA-tagged microcapsule in water. The line curve corresponds to two Gaussian function fits, and the shell thickness was taken at the full width at half maximum. (f) Scanning electron microscopy image, in secondary electrons mode, of microcapsules obtained after drying water-in-chloroform dispersions. (g) Acetalization crosslinking reaction product between PVA and glutaraldehyde. (h) Kinetic profile of the crosslinking reaction on microcapsules as measured by the decrease of aldehyde characteristic signal using ^{1}H NMR. (i) Cumulative cargo release profiles of pristine and crosslinked microcapsules as measured by UV-visible spectroscopy. Lines are guides for the eye. Scale-bars represent 50 μm, unless otherwise indicated.

at 0.02 equiv -CHO /equiv -OH (Table S3), providing sufficient shell crosslinking while minimizing interparticle crosslinking and thus avoiding aggregation.

Cargo release was studied using a small hydrophilic dye, i.e. methyl blue, an organic polyanion of M_w = 800 g mol^{-1}. It was encapsulated in PVA capsule following route (1), Fig. 1 (for experimental details, refer to SI and Fig S9). After solvent transfer to salted water, the capsules were let releasing their cargo at room temperature under agitation. The release profiles of pristine and crosslinked capsules are reproduced in Fig 3g. At t = 0, the cargo released amount is already at ca. 20%. This is probably due to the breaking down of a substantial number of capsules during solvent transfer. For t < 3 h, the high slope of the curves reveal a fast release (burst effect). Then, the release gets faster for pristine capsules at t > 3 h. This increase of the release rate was associated to the experimentally observed dissolution of the capsule twisted by shear. On the contrary, the release gets slower for crosslinked capsules at t > 3 h, since the capsules did not dissolve in this case. The slope in $t^{1/2}$ suggests a diffusion-controlled release (regression over five points: R^2 > 0.998). The full completion of cargo release from pristine capsules was reached between 6 and 24 h (most of the capsules were completely dissolved after 24 h), whereas only ca. 50% was released from crosslinked capsule after 48 h. Remarkably, the final release value from pristine capsule was close to 100%, suggesting a quantitative encapsulation yield.

We have seen that PVA\80-10 stabilizes both o/w and w/o dispersions, depending on temperature. This unique behavior was further exploited to create multiple dispersions using the same polymer. For the proof-of-concept of route (2), Fig 1, we used a water-immiscible oil presenting a high polarity and a low vapor pressure, ethyl acetoacetate (see corresponding phase diagram in Fig S10). First, coacervated w/o dispersions were prepared by emulsification of PVA\80-10 solution and ethyl acetoacetate (20:80, v:v) at 50 °C using sonication (cf. SEM micrographs in Fig S11). Then, a large volume (80:20, v:v) of the same PVA solution was added and a second emulsification performed using magnetic agitation at 25 °C. PVA\80-10 stabilizes the thus-formed w/o/w multiple dispersion. To illustrate this, we spiked the water and oil phases with a hydrophilic (green-emitting) and a hydrophobic fluorophore (red-emitting), respectively (see Fig 4a-c). We clearly observe the separated fluorescence signals, showing that oil bigger capsules are mostly embedded with one or several smaller water-filled capsules, with respective average diameters around 28 µm and 8 µm (Fig S7). With a new emulsification step in oil at 50 °C, one likely yields triple w/o/w/o dispersions in a single pot (Fig S12).

As a preliminary move towards application, we applied the process of route (2) to the encapsulation of anticancer drugs, knowing that PVA is already FDA-approved. We selected α-terpineol as a therapeutic and bioderived oil, known for its antitumor activity.[17] As for anticancer drugs, hydrophilic doxorubicin hydrochloride and hydrophobic paclitaxel were respectively coencapsulated in water- and oil-filled microcapsules of w/o/w dispersions. High loading of separate pools of drugs, not intermixing, were observed in the microcapsules, as shown in Fig 4d-f. Interestingly, our coencapsulation process is advantageous over the previously reported ones,[18] because it does not necessary involve a crosslinking reaction nor requires the use of metal ions.

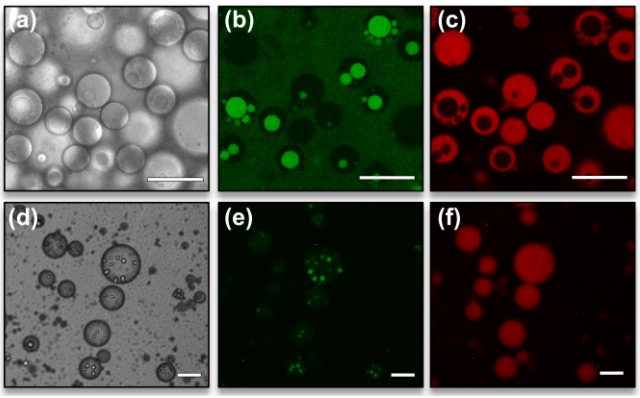

Figure 4. (a) Transmission confocal microscopy image of a water-in-oil-in-water dispersion, with its according fluorescence images (b) hydrophilic domains and (c) hydrophobic domains. (oil: ethyl acetoacetate). (d) Transmission microscopy of a water-in-oil-in-water dispersion with its according reflection fluorescence images (e) hydrophilic domains loaded with doxorubicin hydrochloride and (f) hydrophobic domains loaded with paclitaxel. (oil: α-terpineol). Scale-bars represent 50 µm.

To conclude, in this communication, we demonstrated that a specific PVA dispersant, which is commercially available, can be used to stabilize both direct and inverse oil/water interfaces. By adding salt and increasing the temperature above the dispersant LCST, this polymer coacervates at water/oil interfaces, forming metastable hollow microcapsules. Diverse fluorophores, dyes and drugs were successfully encapsulated in quantitative yields. A diffusion-controlled release was observed for covalently crosslinked capsules. Also, multiple dispersions were synthesized using a remarkably simple protocol, enabling an easy hydrophilic/hydrophobic anticancer drugs microencapsulation. Further research aims at better mastering this process by looking at the impact of polymer microstructure on solution behavior and structuration in the shell. We also seek new bio-based dispersants with similar properties.

ASSOCIATED CONTENT

Supporting Information. Experimental details. NMR spectra. DLS plots. DSC thermograms. XRD diffractograms. Object size distribution histograms. Calibration curves. The Supporting Information is available free of charge on the ACS Publications website.

AUTHOR INFORMATION

Corresponding Author

François Ganachaud. Francois.ganachaud@insa-lyon.fr.

ACKNOWLEDGMENT

Lérys Granado thanks the French-American Chamber of Commerce and Business France for the sponsorship of international exchange. The authors thank Synthomer for kindly providing polyvinyl alcohol samples. Dr J. Bernard is acknowledged for helpful discussions and corrections.

REFERENCES

(1) De Cock, L. J.; De Koker, S.; De Geest, B. G.; Grooten, J.; Vervaet, C.; Remon, J. P.; Sukhorukov, G. B.; Antipina, M. N. Polymeric Multilayer Capsules in Drug Delivery. *Angew. Chemie - Int. Ed.* **2010**, *49* (39), 6954–6973.

(2) Lin, C. T.; Lin, I. C.; Sung, S. Y.; Su, Y. L.; Huang, Y. F.; Chiang, C. S.; Hu, S. H. Dual-Targeted Photopenetrative Delivery of Multiple Micelles/Hydrophobic Drugs by a Nanopea for Enhanced Tumor Therapy. *Adv. Funct. Mater.* **2016**, *26* (23), 4169–4179.

(3) McClements, D. J. Encapsulation, Protection, and Release of Hydrophilic Active Components: Potential and Limitations of Colloidal Delivery Systems. *Adv. Colloid Interface Sci.* **2015**, *219*, 27–53.

(4) Li, Q.; Li, X.; Zhao, C. Strategies to Obtain Encapsulation and Controlled Release of Small Hydrophilic Molecules. *Front. Bioeng. Biotechnol.* **2020**, *8* (May), 1–6.

(5) Musyanovych, A.; Landfester, K. Polymer Micro- and Nanocapsules as Biological Carriers with Multifunctional Properties. *Macromol. Biosci.* **2014**, *14* (4), 458–477.

(6) Lu, H. D.; Rummaneethorn, P.; Ristroph, K. D.; Prud'Homme, R. K. Hydrophobic Ion Pairing of Peptide Antibiotics for Processing into Controlled Release Nanocarrier Formulations. *Mol. Pharm.* **2018**, *15* (1), 216–225.

(7) (A) Wald, S.; Wurm, F.; Landfester, K.; Crespy, D. Stabilization of Inverse Miniemulsions by Silyl-Protected Homopolymers. *Polymers (Basel).* **2016**, *8* (8), 303. (B) Anton, N.; Saulnier, P.; Gaillard, C.; Porcher, E.; Vrignaud, S.; Benoit, J.-P. Aqueous-Core Lipid Nanocapsules for Encapsulating Fragile Hydrophilic and/or Lipophilic Molecules. *Langmuir* **2009**, *25* (19), 11413–11419.

(8) Teodorescu, M.; Bercea, M.; Morariu, S. Biomaterials of Poly(Vinyl Alcohol) and Natural Polymers. *Polym. Rev.* **2018**, *58* (2), 247–287.

(9) Congdon, T.; Shaw, P.; Gibson, M. I. Thermoresponsive, Well-Defined, Poly(Vinyl Alcohol) Co-Polymers. *Polym. Chem.* **2015**, *6* (26), 4749–4757.

(10) Eagland, D.; Crowther, N. J. Influence of Composition and Segment Distribution upon Lower Critical Demixing of Aqueous Poly(Vinyl Alcohol-Stat-Vinyl Acetate) Solutions. *Eur. Polym. J.* **1991**, *27* (3), 299–301.

(11) Bachtsi, A. R.; Boutris, C. J.; Kiparissides, C. Production of Oil-Containing Crosslinked Poly(Vinyl Alcohol) Microcapsules by Phase Separation: Effect of Process Parameters on the Capsule Size Distribution. *J. Appl. Polym. Sci.* **1996**, *60* (1), 9–20.

(12) Kiyama, K. Applications of Polyvinyl Alcohol Microcapsules. In *Novel Cosmetic Delivery Systems*; Dekker, M., Ed.; 1998; pp 315–331.

(13) Alves, M.-H.; Jensen, B. E. B.; Smith, A. A. A.; Zelikin, A. N. Poly(Vinyl Alcohol) Physical Hydrogels: New Vista on a Long Serving Biomaterial. *Macromol. Biosci.* **2011**, *11* (10), 1293–1313.

(14) Hu, S. H.; Liao, B. J.; Chiang, C. S.; Chen, P. J.; Chen, I. W.; Chen, S. Y. Core-Shell Nanocapsules Stabilized by Single-Component Polymer and Nanoparticles for Magneto-Chemotherapy/Hyperthermia with Multiple Drugs. *Adv. Mater.* **2012**, *24* (27), 3627–3632.

(15) Mačiulyte, S.; Gutauskiene, G.; Niedritis, J.; Kochane, T.; Budriene, S. PVA and Various Diisocyanates Based Poly(Urethane-Urea) Microcapsules for Encapsulation of Enzyme in Water/Butyl Acetate Emulsion: Synthesis and Study. *Chemija* **2017**, *28* (1), 74–84.

(16) Budhlall, B. M.; Landfester, K.; Sudol, E. D.; Dimonie, V. L.; Klein, A.; El-Aasser, M. S. Characterization of Partially Hydrolyzed Poly(Vinyl Alcohol). Effect of Poly(Vinyl Alcohol) Molecular Architecture on Aqueous Phase Conformation. *Macromolecules* **2003**, *36* (25), 9477–9484.

(17) Khaleel, C.; Tabanca, N.; Buchbauer, G. α-Terpineol, a Natural Monoterpene: A Review of Its Biological Properties. *Open Chem.* **2018**, *16* (1), 349–361.

(18) Liu, Y.; Fang, J.; Kim, Y.-J; Wong, M. K.; Wang, P. Codelivery of Doxorubicin and Paclitaxel by Cross-Linked Multilamellar Liposome Enables Synergistic Antitumor Activity. *Mol. Pharmaceutics* **2014**, *11* (5), 1651–1661.

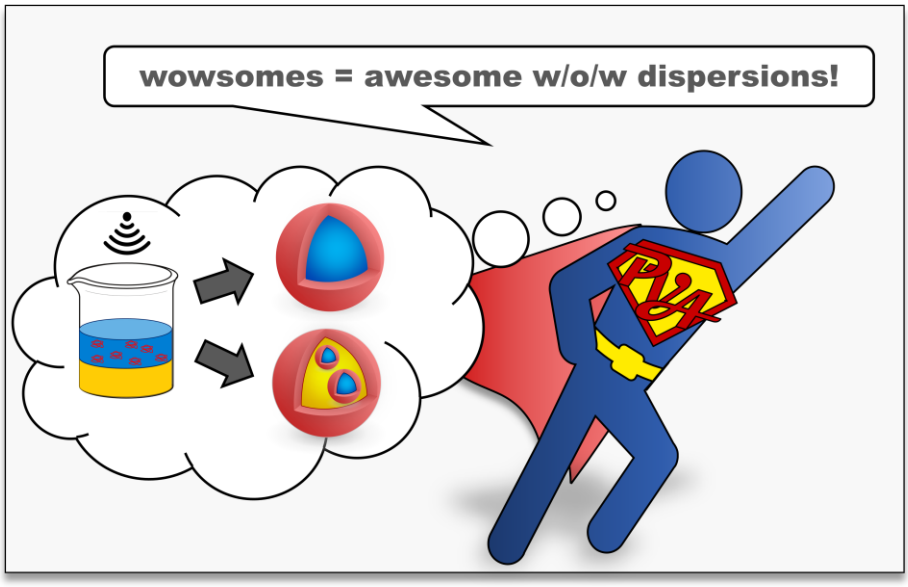
wowsomes = awesome w/o/w dispersions!